PROCEEDINGS OF SCIENCE

Fermi-LAT Detection of a GeV Afterglow from a Compact Stellar Merger

Hai-Ming Zhang,[a,b,*] **Yi-Yun Huang,**[a,b] **Jian-He Zheng,**[a,b] **Ruo-Yu Liu**[a,b] **and Xiang-Yu Wang**[a,b]

[a] *School of Astronomy and Space Science, Nanjing University, Nanjing 210023, China*
[b] *Key laboratory of Modern Astronomy and Astrophysics (Nanjing University), Ministry of Education, Nanjing 210023, China*

E-mail: hmzhang@nju.edu.cn, ryliu@nju.edu.cn, xywang@nju.edu.cn

It is usually thought that the long-duration (>2 s) gamma-ray bursts (GRBs) are associated with massive star core collapse, however the short-duration (<2 s) GRBs are associated with mergers of compact stellar binaries. In this work, we report the Fermi-LAT detection of gamma-ray (> 100 MeV) afterglow emission from GRB 211211A, which is a nearby (350 Mpc) long-duration GRB but discovered as a kilonova association. The gamma-ray emission from GRB 211211A lasts ~20,000 s after the burst, which suggests that it is the longest event for conventional short-duration GRBs ever detected. We suggest that this gamma-ray emission results from afterglow synchrotron emission. The soft spectrum of GeV emission may arise from a limited maximum synchrotron energy of only a few hundreds of MeV at ~20,000 s. The usually long duration of the GeV emission could be due to the proximity of this GRB and the long deceleration time of the GRB jet that is expanding in a low-density circumburst medium, consistent with the compact stellar merger scenario.

38th International Cosmic Ray Conference (ICRC2023)
26 July - 3 August, 2023
Nagoya, Japan

*Speaker

PoS(ICRC2023)887

1. Introduction

Gamma-ray bursts (GRBs) are usually divided into two populations [1]: long GRBs that originate from the core collapse of massive stars [2] and short GRBs formed in the merger of two compact objects [3]. While it is common to divide the two populations at a duration of 2 s for the prompt keV/MeV emission, classification based on duration only does not always correctly point to the progenitor. The emission of GRBs can be divided into two stages. One is prompt emission, whose light curve is very intense and is believed to be resulted from internal shocks or other dissipation mechanisms that occur at small radii. The other is afterglow, whose light curve shows power-law decays in time and is believed to originate from external shocks. There are some peculiar GRBs, such as GRB 060614, reported long-duration burst and was associated with a kilonova-like feature [4]. Growing observations [5] have shown that multiple criteria (such as supernova/kilonova associations and host galaxy properties) rather than burst duration only are needed to classify GRBs physically.

GRB 211211A triggered the Burst Alert Telescope (BAT; [6]) on board the Neil Gehrels Swift Observatory at 13:09:59 UT [7], the Gamma-ray Burst Monitor (GBM; [8]) on board the Fermi Gamma-Ray Space Telescope at 13:09:59.651 UT [9] and High energy X-ray Telescope on board Insight-HXMT [10] at 13:09:59 UT on 2021 December 11. The burst is characterized by a spiky main emission phase lasting ~13 s, and a longer, weaker extended emission phase lasting ~55 s [11]. The prompt emission is suggested to be produced by the fast-cooling synchrotron emission [12]. The discovery of a kilonova associated with this GRB indicates clearly that the progenitor is a compact object merger [13]. The event fluence (10-1000 keV) of the prompt emission is $(5.4 \pm 0.01) \times 10^{-4}$ erg cm^{-2}, making this GRB an exceptionally bright event. The host galaxy redshift of GRB 211211A is $z = 0.0763 \pm 0.0002$ (corresponding to a distance of ≈350 Mpc; [13]). Zhong, Li, & Dai [14] suggests that this association event may arise from a neutron star-white dwarf (NS-WD) merger.

2. Fermi-LAT data analysis

At 13:09:59 UT (denoted as T_0), the Swift/BAT triggered and located GRB 211211A [7]. The Fermi-LAT extended type data for the GRB 211211A was taken from the Fermi Science Support Center[1] from $T_0 - 10$ days to $T_0 + 10$ days. We select the observation time of GRB 211211A by LAT only when the angle from the Fermi-LAT boresight is less than 100°. The first observation starts at 395 s after Swift/BAT trigger, so we use the Source-class event selection, which has more stringent background rejection cuts than Transient-class events and is better suited for analyses of long time intervals and dimmer sources. The instrument response functions (IRFs; P8R3_SOURCE_V3) is used. The data analysis was performed using the publicly available software fermitools (ver. 2.0.8) with the unbinned likelihood analysis method. The maximum likelihood test statistic (TS) is used to estimate the significance of the GRB, which is defined by TS= $2(\ln \mathcal{L}_1 - \ln \mathcal{L}_0)$, where $\mathcal{L}_1$ and $\mathcal{L}_0$ are maximum likelihood values for the background with the GRB and without the GRB (null hypothesis).

[1] https://fermi.gsfc.nasa.gov

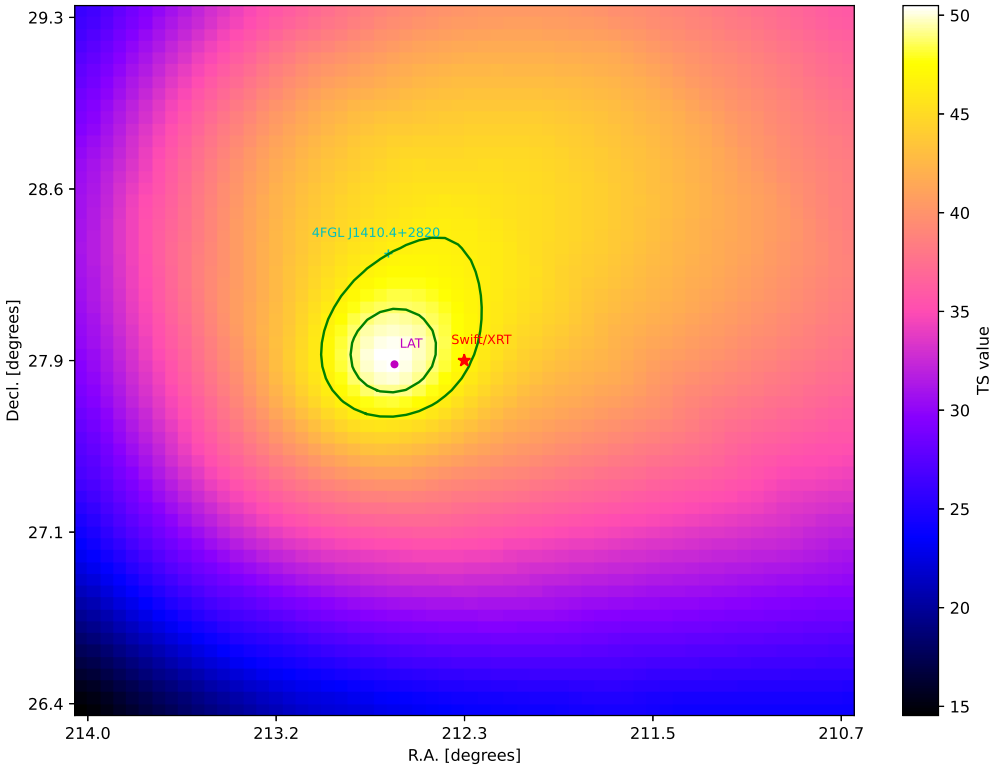

Figure 1: $3^\circ \times 3^\circ$ TS map of the gamma-ray emission in 0.1–10 GeV measured by Fermi-LAT around GRB 211211A in 395–30780 s after the BAT trigger [16]. The cyan cross represents 4FGL J1410.4+2820, which is suggested to be associated with a BL Lacertae RX J1410.4+2821 by Fermi-LAT Collaboration [15]. The magenta point indicates the best localization of GRB 211211A. The two green lines represent the localization contours of GRB 211211A at 68% and 90% confidence levels, respectively. The red star represents the localization of GRB 211211A by Swift/XRT [7].

3. Results

Using the gttsmap tool, we evaluate the TS map in the vicinity of the GRB, which is shown in Figure 1 [16]. The maximum value, $\mathrm{TS_{max}} = 50.82$ corresponds to a detection significance of 6.2σ or 6.7σ (one-sided) if the $\mathrm{TS_{max}}$ distribution follows $(1/2)\chi^2_4$ or $(1/2)\chi^2_2$, respectively. We compute the error contours of the source localization using the method suggested by [17], and the iso-contours containing localization probabilities of 68% and 90% are shown as green lines in Figure 1. We find that the GRB position detected by Swift is inside the region of the localization contours of LAT at the 90% confidence level. We note that one 4FGL source (4FGL J1410.4+2820) is close to the GRB ($0^\circ.55$ from Swift/XRT position). We estimate its $\sim$ 13.3 years average flux before the GRB trigger to be $(1.59 \pm 0.41) \times 10^{-9}$ photons cm^{-2} s^{-1} (the light curve of 4FGL J1410.4+2820 is shown in Figure 2 [16]). This flux implies that this source is not bright enough to be considered as the background source in the model.

We use the gtsrcprob tool to estimate the probability that each photon detected by the LAT is associated with the GRB. The list of events associated with the GRB with a probability higher than 80% is shown in Table 1 [16], among which six photons have the probability higher than 90%. The

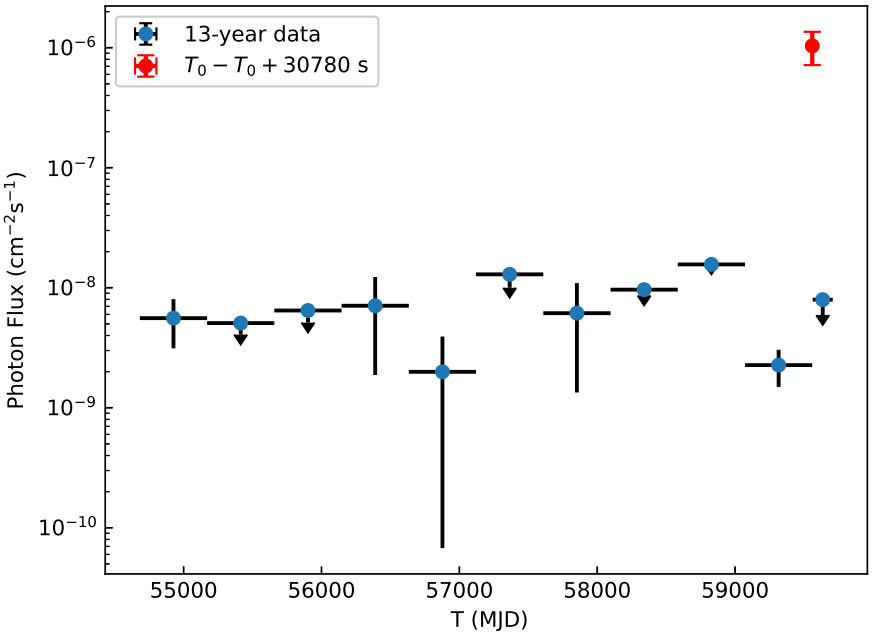

Figure 2: Light curve of 4FGL J1410.4+2820 in 0.1-10 GeV (blue data) in comparison with the GeV flux (red data) from GRB 211211A [16].

first γ-ray photon with the probability exceeding 90% arrives at $T_0 + 6438.83$ s, with an energy of 206.91 MeV, and the highest-energy photon is a 1740.45 MeV photon arriving at $T_0 + 12967.39$ s.

Table 1: List of the selected gamma-ray events with a probability of association > 80% in 395-30780 s [16].

Time since T_0 (s)	Energy(MeV)	R.A.(deg)	Decl.(deg)	Probability(%)
1165.89	400.05	213.28	27.25	86.80
6238.33	142.38	212.64	29.01	84.18
6438.83	206.91	212.67	27.82	90.42
6648.08	187.58	212.11	28.91	90.91
12494.06	163.96	212.57	29.20	89.95
12967.39	1740.45	212.63	27.85	98.91
13054.08	102.64	211.48	28.20	94.41
17410.06	113.83	211.61	27.22	92.45
17861.10	286.10	213.34	28.65	88.36
18128.17	231.49	212.80	28.36	94.83
24487.04	104.01	214.33	29.19	88.31
28335.50	274.59	212.37	26.89	88.35

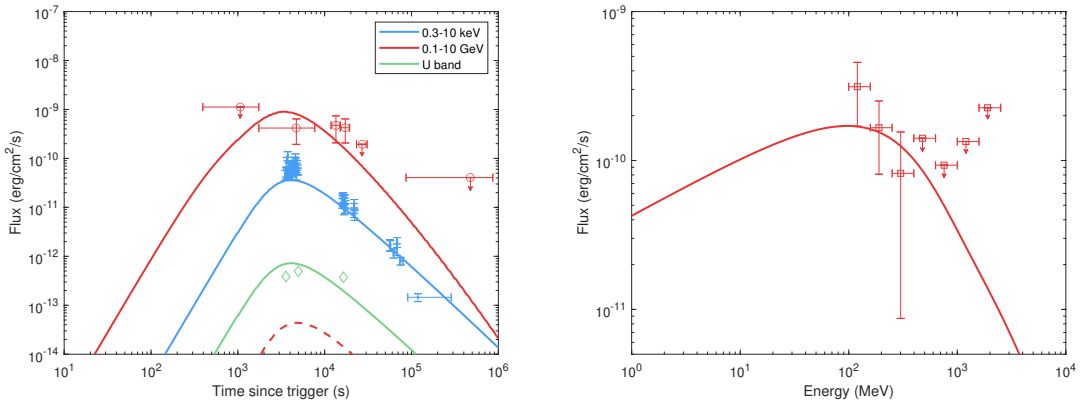

Figure 3: Left panel: light curves of the GeV emission of GRB 211211A measured by Fermi-LAT and the modeling of the multi-wavelength afterglow light curves [16]. The red, blue and green data points represent the GeV, X-ray and early optical flux of GRB 211211A, respectively. X-ray data are downloaded from the UK Swift Science Data Centre (UKSSDC). The optical data are obtained from [13]. The solid lines represent the synchrotron emission at GeV, X-ray and optical bands, while the dashed line represents the SSC component at the GeV band in our modeling. Right panel: the measured spectrum and modeling of the GeV emission of GRB 211211A during 395–30780 s [16]. The parameters used in the modeling are $E_{\rm k,iso} = 1 \times 10^{53}$ erg, $\Gamma_0 = 100$, $n = 10^{-4}$ cm^{-3}, $p = 2.2$, $\varepsilon_{\rm e} = 0.1$, $\varepsilon_{\rm B} = 6 \times 10^{-5}$, $\theta_{\rm j} = 1.0^\circ$ and $\eta_{\rm acc} = 0.01$ (see the text for more details).

4. Interpretation of the GeV emission

The maximum energy of the photons detected from GRB 211211A is only 1.7 GeV, so it is reasonable to consider the afterglow synchrotron emission scenario. Below we study the possibility of the forward shock emitting the GeV afterglow emission. As shown in Figure 3 [16], we perform modeling of the Fermi-LAT data for GRB 211211A using a numerical code developed in our previous work [18]. According to the standard afterglow model [19], the light curve for a given observed frequency (ν) could be calculated as $F(t,\nu) = F(t,\nu,E_{\rm k,iso},n,p,\varepsilon_{\rm e},\varepsilon_{\rm B},\Gamma_0,\theta_{\rm j})$. Here $E_{\rm k,iso}$ is the isotropic kinetic energy of the GRB outflow, n is the particle number density of the ambient medium, p is the electron spectral index, $\varepsilon_{\rm e}$ and $\varepsilon_{\rm B}$ are the equipartition factors for the energy in electrons and magnetic field in the shock, Γ_0 is the initial Lorentz factor of the outflow, and $\theta_{\rm j}$ is the half-opening angle of the jet. In this code, the electrons that produce synchrotron high-energy emission also undergo IC loss and the Klein–Nishina (KN) effect has been taken into account [20]. We find that the model can reproduce the light curves of GeV and X-ray afterglows, as well as the optical afterglow at early time when the kilonova emission is subdominant [13], for the following parameter values: $E_{\rm k,iso} = 1 \times 10^{53}$ erg, $\Gamma_0 = 100$, $n = 10^{-4}$ cm^{-3}, $p = 2.2$, $\varepsilon_{\rm e} = 0.1$, $\varepsilon_{\rm B} = 6 \times 10^{-5}$ and $\theta_{\rm j} = 1.0^\circ$ (see Figure 3). The measured photon index of the X-ray afterglow by Swift/XRT ($\Gamma_{\rm X} = -1.5^{+1.2}_{-0.06}$; [21]) is also consistent with $p = 2.2$, as the X-ray frequency locates in the regime $\nu_m < \nu_{\rm X} < \nu_c$, where ν_m and ν_c are, respectively, the frequencies corresponding to the injection break and cooling break [19]. We note that the observed X-ray flux at 3-5 ks exceeds the model flux to some extent, which could indicate that the early X-ray emission may have some contribution from an extra component other than the afterglow, such as the central engine activity,

as have been seen in some GRB X-ray afterglows [22].

To explain the long-duration of the GeV emission, a long deceleration time for the external shock is needed. This implies a low density of $n \simeq 10^{-4}\,\mathrm{cm}^{-3}$. Such a low density of the ambient medium is not surprising, since the GRB lies outside of the optical disk of the host galaxy, consistent with the compact stellar merger scenario. In addition, Quasi-Periodic Oscillations (QPO) with frequency $\simeq 22$ Hz are found throughout the precursor of GRB 211211A [10], which indicates most likely that a magnetar participated in the merger. The pulsar wind from the magnetar may have created a cavity around the pulsar [23].

5. Summary

We reported the detection of a GeV afterglow from GRB 211211A, which is a long-duration GRB, but results from a compact stellar merger. The GeV emission continues up to about 20,000 s after the burst. The duration is the longest one compared to the GeV afterglows of other short-duration GRBs. Since GRB 211211A occurs at the position outside the galaxy disk, the density of the circumburst medium is expected to be low, which leads to a subdominant contribution to the GeV emission by the SSC component. Instead, we find that the GeV emission of GRB 211211A can be interpreted as arising from the afterglow synchrotron emission. The soft spectrum of the GeV emission could arise from a limited maximum synchrotron energy of only a few hundreds of MeV at $\sim 20,000$ s. The long duration of the GeV emission can be interpreted as the long deceleration time due to a low-density circumburst environment, which agrees well with the density environment expected for compact stellar mergers.

Acknowledgments

The work is supported by the NSFC Grants No. 12203022, No.12121003 and No. U2031105, the Natural Science Foundation of Jiangsu Province grant BK20220757.

References

[1] Norris J. P., Cline T. L., Desai U. D., Teegarden B. J., 1984, Natur, 308, 434. doi:10.1038/308434a0

[2] Galama T. J., Vreeswijk P. M., van Paradijs J., Kouveliotou C., Augusteijn T., Böhnhardt H., Brewer J. P., et al., 1998, Natur, 395, 670. doi:10.1038/27150

[3] Abbott B. P., Abbott R., Abbott T. D., Acernese F., Ackley K., Adams C., Adams T., et al., 2017, ApJL, 848, L12. doi:10.3847/2041-8213/aa91c9

[4] Yang B., Jin Z.-P., Li X., Covino S., Zheng X.-Z., Hotokezaka K., Fan Y.-Z., et al., 2015, NatCo, 6, 7323. doi:10.1038/ncomms8323

[5] Zhang B.-B., Liu Z.-K., Peng Z.-K., Li Y., Lü H.-J., Yang J., Yang Y.-S., et al., 2021, NatAs, 5, 911. doi:10.1038/s41550-021-01395-z

[6] Barthelmy S. D., Barbier L. M., Cummings J. R., Fenimore E. E., Gehrels N., Hullinger D., Krimm H. A., et al., 2005, SSRv, 120, 143. doi:10.1007/s11214-005-5096-3

[7] D'Ai A., Ambrosi E., D'Elia V., Gropp J. D., Kennea J. A., Kuin N. P. M., Lien A. Y., et al., 2021, GCN, 31202

[8] Meegan C., Lichti G., Bhat P. N., Bissaldi E., Briggs M. S., Connaughton V., Diehl R., et al., 2009, ApJ, 702, 791. doi:10.1088/0004-637X/702/1/791

[9] Mangan J., Dunwoody R., Meegan C., Fermi GBM Team, 2021, GCN, 31210

[10] Xiao S., Zhang Y.-Q., Zhu Z.-P., Xiong S.-L., Gao H., Xu D., Zhang S.-N., et al., 2022, arXiv, arXiv:2205.02186. doi:10.48550/arXiv.2205.02186

[11] Yang J., Ai S., Zhang B.-B., Zhang B., Liu Z.-K., Wang X. I., Yang Y.-H., et al., 2022, Natur, 612, 232. doi:10.1038/s41586-022-05403-8

[12] Gompertz B. P., Ravasio M. E., Nicholl M., Levan A. J., Metzger B. D., Oates S. R., Lamb G. P., et al., 2023, NatAs, 7, 67. doi:10.1038/s41550-022-01819-4

[13] Rastinejad J. C., Gompertz B. P., Levan A. J., Fong W.-. fai ., Nicholl M., Lamb G. P., Malesani D. B., et al., 2022, Natur, 612, 223. doi:10.1038/s41586-022-05390-w

[14] Zhong S.-Q., Li L., Dai Z.-G., 2023, ApJL, 947, L21. doi:10.3847/2041-8213/acca83

[15] Abdollahi S., Acero F., Ackermann M., Ajello M., Atwood W. B., Axelsson M., Baldini L., et al., 2020, ApJS, 247, 33. doi:10.3847/1538-4365/ab6bcb

[16] Zhang H.-M., Huang Y.-Y., Zheng J.-H., Liu R.-Y., Wang X.-Y., 2022, ApJL, 933, L22. doi:10.3847/2041-8213/ac7b23

[17] Fermi-LAT Collaboration, Ajello M., Atwood W. B., Axelsson M., Baldini L., Barbiellini G., Baring M. G., et al., 2021, NatAs, 5, 385. doi:10.1038/s41550-020-01287-8

[18] Liu R.-Y., Wang X.-Y., Wu X.-F., 2013, ApJL, 773, L20. doi:10.1088/2041-8205/773/2/L20

[19] Sari R., Piran T., Narayan R., 1998, ApJL, 497, L17. doi:10.1086/311269

[20] Wang X.-Y., He H.-N., Li Z., Wu X.-F., Dai Z.-G., 2010, ApJ, 712, 1232. doi:10.1088/0004-637X/712/2/1232

[21] Osborne J. P., Page K. L., Ambrosi E., Capalbi M., Perri M., Burrows D. N., Gropp J. D., et al., 2021, GCN, 31212

[22] Troja E., Cusumano G., O'Brien P. T., Zhang B., Sbarufatti B., Mangano V., Willingale R., et al., 2007, ApJ, 665, 599. doi:10.1086/519450

[23] Holcomb C., Ramirez-Ruiz E., De Colle F., Montes G., 2014, ApJL, 790, L3. doi:10.1088/2041-8205/790/1/L3